39th IAHR WORLD CONGRESS
GRANADA, SPAIN 2022
From Snow to Sea
19-24 June 2022

Proceedings of the 39th IAHR World Congress
19-24 June 2022
Granada, Spain
DOI number

Assessing the Sensitivity of Tidal Range Energy Models to Water Level Accuracy

Nicolas Hanousek[(1)], Reza Ahmadian[(2)]

[(1)] Cardiff University School of Engineering, Cardiff, United Kingdom, HanousekN@Cardiff.ac.uk
[(2)] Cardiff University School of Engineering, Cardiff, United Kingdom, AhmadianR@Cardiff.ac.uk

Abstract

Tidal range energy has long been considered for contribution to a low-carbon electricity mix, with schemes in operation for over half a century, generating dispatchable, predictable, energy. Proposed schemes are often modelled using simplified 0D models in the optimisation stages, taking a few key inputs to describe the operation of a tidal range scheme. Fundamental among these is the external water level, typically extracted from other models or harmonic extraction. To assess the possible variation in energy outputs that can be incurred from an erroneous water level, a set of base outputs for two tidal range schemes were determined using a combination of configurations. A set of error forms were identified, applied to the base water levels, and statistical parameters identified from the literature used to provide a set of erroneous water level sets within the reported accuracy. The tidal range schemes were then run using these mutated time series and the change in performance to the base condition was calculated. The models showed significant change in financial yield for the period with the error passing the criteria previously used, demonstrating the need for additional methods to assess the errors. The tests found that the tidal range schemes do not have a particular operating mode that is more resilient or susceptible to an inaccurate water level series, although, of the chosen schemes, one was more varied, indicating that future work may indicate a physical characteristic leading to a more consistent energy estimate.

Keywords: Renewable Energy; Tidal Energy; Sensitivity Analysis; 0D Modelling

1. INTRODUCTION

1.1 Tidal Range Energy

Driven by a global need for low-carbon electricity, sources of potentially underutilized power are being explored as an opportunity to contribute to a diverse energy generation mix. Advances and new technologies, along with this ever-increasing drive to generate clean energy open the door to alternative methods of generation. Tidal range energy has been providing reliable and dispatchable energy since the first scheme came online at La Rance in France in the 1960s, where it has produced energy consistently since the 1960s producing approximately 480 GWh of electricity per year (Rtimi et al., 2021). Newer schemes in China, Russia and Canada have since been constructed, with the world's largest and most recent scheme being built in Incheon, South Korea in 2011 (Neill et al., 2018). Tidal range schemes have been considered for construction in the United Kingdom for over a century, however, the high capital expenditure and environmental concerns have resulted in most proposals eventually stalling out (Waters and Aggidis, 2016). In recent years, there has been an uptick in interest in tidal range, and the advantages that this energy form can offer over other renewables (Ahmadian and Hanousek, 2021; Swansea Council, 2021).

A tidal range energy scheme generates electricity by harnessing the rising and falling of the water level due to the tides. To achieve this, an area is isolated from the open water system, connected by a combination of sluice gates and turbines. Water is held in the internal area until a suitable difference is achieved across the structure, and the turbines then opened to allow the water across, until the difference is so small that the energy generation is no longer beneficial, at which point the sluice gates are opened to allow a greater degree of flow; in parallel sluicing (referred to by Moreira et al. (2022) as 'variant operation') the sluices are opened before the generation period has finished, accelerating the process of filling or draining the lagoon. Once the water level has reached a maximum (or minimum) within the scheme, the sluice gates (and turbines) are closed to prevent water from passing through and allow the external tide to develop a head difference once again. This forms a cyclical series of operating modes, described in Table 1. Pumping can be used before the holding stage to accentuate the internal tidal range and has been shown to increase in yields, as relatively cheap low head pumping leads to the generation phase occurring under beneficial conditions in the following period. A schematic of the internal and external water levels along is shown in Figure 1. The process of generation can be carried

out on either the falling (ebbing) tidal period, the rising (flooding) tide, or on both. Of these, the most considered are Ebb-Only and Two-Way with Flood-Only operation only being in use at the Lake Sihwa scheme in Korea, where maintaining a lower internal water level is a design factor (Neill et al., 2018).

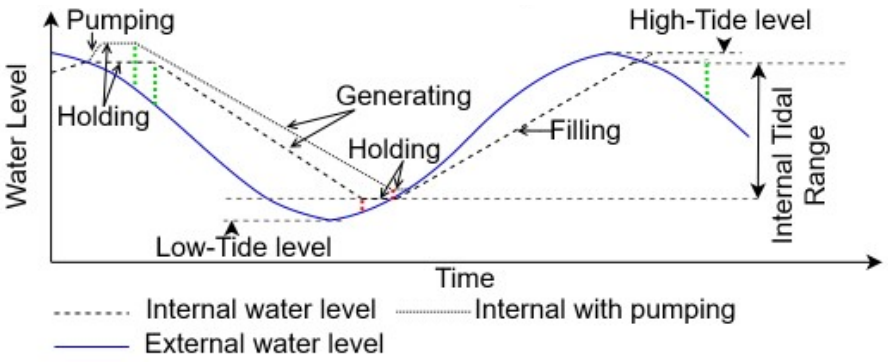

Figure 1. Outline ebb-only tidal range scheme operation.

Table 1. Tidal range scheme behaviour during different operating phases.

MODE	SLUICE FLOW	TURBINE FLOW	POWER
Holding	None	None	None
Generating	None	Open	Producing
Sluicing (Serial)	Open	Closed	None
Sluicing (Parallel)	Open	Open	Producing
Pumping	Closed	Forced	Consuming

Although a tidal range scheme is primarily an energy device, due to the ability to vary the start and end head differences, a TRS can have some control over the timing of generation to match preferred performance. Harcourt et al. (2019) found that flexible timing could yield an increase in profit of 1-9%, even with a reduced net energy output by 2-14%. This is beneficial to the network as a while, as the variability of intermittent renewables can have undesirable effects on a national grid (Rehman et al., 2015) where unexpected weather events can lead to imbalances in the system. The energy market in the UK varies both on an annual scale due to seasonal demands, and on a daily scale as shown in Figure 2, normalised to the annual mean price, data from Elexon (2020). As such, the modelling carried out here is focused on profit as opposed to energy output. Achieving an accurate prediction of the potential energy output or financial yield is critical to a project of this size due to the high capital expenditure. A difference in output of a few percent can be the balance point of financial viability, as has kept proposals such Swansea Bay from being carried on to fruition (Waters and Aggidis, 2016).

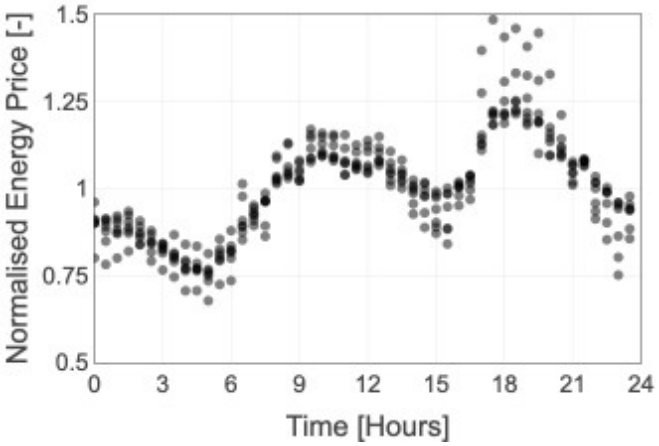

Figure 2. UK national grid daily average energy prices from 2012-2018

1.2 Modelling Approaches

Due to the size and scale of a tidal range energy scheme, the potential environmental impact and financial outlay require that the operation of a proposed scheme is thoroughly understood before it can be commissioned. In aid of this, modelling approaches are used to represent the scheme and carry out both investigations into the impacts of a given operation and optimise the operational choices used to maximise outputs. One increasingly common method to do this is the use of 0-dimensional (0D) models, as used by Todeschini et al. (2021), Harcourt et al. (2019), Xue et al. (2019) and others.

0D models use a relationship-based representation of the tidal range scheme to determine how it will operate under a given set of design choices, operational decisions, and external water levels. This allows for a computationally low-cost assessment of the scheme when compared to the requirement to solve even simplified formulations of the Navier-Stokes equations across a complex numerical domain. A 0D model takes an external time series of water level, obtained from either a measurement of appropriate site data, extracted from a calibrated larger-domain model, or forecast from tidal constituents at the chosen site. This fluid time series is then linked to an area (the impounded area of the scheme) whose water level rises and falls based on the inflow and outflow, primarily governed by the flow across the sluices and turbines as described in Table 1. The trigger points for the start and end of generation are the 'starting' and 'ending' heads, these can either be set to fixed values for a given period or changed at relevant intervals to allow the scheme to best utilise the variations in the tidal trace, known as flexible operation. Flexible operation has been found to provide an improved output in comparison to fixed, and there are a variety of methods for ascertaining the levels to be used. In this study, the Every Half Next (EHN) principle as described by Xue et al. (2019) was employed.

To develop a picture of the level of calibration typically used in numerical modelling studies, 15 peer-reviewed works[a] were found to be relevant; excluding articles that utilise and refer to previously described models, and where multiple values are provided, using the lowest performing. Within these, two major approaches were seen, either a bulk statistical analysis of the time-series at given calibration points, a spectral analysis of the major tidal constituents, or some combination of the two. The most used parameter was the Root Mean Square Error (n = 8) with reported values from 0.08 – 0.53 metres, followed by the R^2 (n = 6) with reported values between 0.86 and 0.997. The Mean Average Error (MAE) was used in two cases. Harmonic constituent analysis typically involved a comparison of the measured and simulated magnitude and phasing of the major components. Williams and Esteves (2017) provide some guidance on the calibration of hydrodynamics models, this suggests using RMSE for water levels along with an analysis of the tidal ranges and the value of carrying out a qualitative assessment of the water levels over the period being assessed.

This study aimed to assess how energy output compared to known errors in the input data, whether a given operational mode of the scheme could be more resilient to errors, what form of error is most easily detected by the metrics, and how the passing errors impact performance.

2. METHOD

2.1 Numerical Model

The 0D model here used the volume V conservation Eq. [1], decomposed to a backward differencing scheme in Eq. [2]. This calculates the internal (upstream) water level η_{up} at a time $n+1$ based on the internal water level at a time n, the inflow to the lagoon from the turbine ($Q_{turbines}$), sluices ($Q_{sluices}$), and environmental inflows from rivers and rainfall etc. (Q_{inflow}), where flows out of the lagoon are positive. The changing area of the scheme $A(\eta)$, over a time step Δt. For this formulation, the flows through the sluices are calculated using an orifice Eq. [3], based on the sluice efficiency coefficient C_D, where the sluices have an area of $A_{sluices}$, and ΔH is the head difference across the scheme (Eq. [4]), g is the gravitational acceleration constant, and δ is a directional operator described in Eq. [5].

$$\frac{dV}{dt} = Q \quad [1]$$

$$\eta_{up}^{n+1} = \eta_{up}^{n} + \frac{(Q_{inflow}^{n} - Q_{sluices}^{n} - Q_{turbines}^{n})}{A(\eta)}\Delta t \quad [2]$$

$$Q_{sluices} = \delta \cdot C_D \cdot A_{sluices} \cdot \sqrt{2g \cdot |\Delta H|} \quad [3]$$

[a] (Moreira et al., 2022; Guo et al., 2021; Mackie et al., 2021; Rtimi et al., 2021; Xue et al., 2019; Ghaedi and Gorginpour, 2021; Xue et al., 2021; Mejia-Olivares et al., 2020; Čož et al., 2019; Angeloudis et al., 2016, 2018; Petley and Aggidis, 2016; Zhou et al., 2014; Aggidis and Benzon, 2013; Xia et al., 2010)

$$\Delta H = \eta_{up} - \eta_{down} \quad [4]$$

$$\delta = \begin{cases} -1, & \Delta H < 0 \\ 1, & \Delta H \geq 0 \end{cases} \quad [5]$$

$$Q_{scaled} = Q_{base} \times \frac{D_{scaled}{}^2}{D_{base}{}^2} \quad [6]$$

Q_{inflow} and η_{down} are both pre-determined and supplied as time-series to the model. The turbine flow rate ($Q_{turbines}$) and power output P are determined using the head difference across the scheme (ΔH), a supplied Hill Chart for the selected turbine design and applied based on the operating mode of the lagoon. This operating mode is determined based on the control parameters, and the prior state of the lagoon. The Hill Chart used in this case is that of an Andritz-Hydro 9m Bulb turbine, of the style used in the majority of existing and proposed schemes, as presented by Aggidis and Feather (2012) and used by numerous subsequent studies. Here slight adjustments are made including a ramping up and down when the turbines start/cease operation, an efficiency adjustment to account for the turbine tending to have better performance in one direction, and a scaling factor to account for the potentially different sizing of the proposed turbine as compared to the base hill-chart (Eq. [6]).

The water level time-series utilised by the tidal range scheme model is typically derived from one of a handful of sources, this can be either a set of historic measurements from a gauging station at a suitable close location, extracted from a 2-dimensional model of a large region (eg: Xue et al. 2021), containing multiple calibration points as well as the site of interest, or constructed based on tidal constituents obtained by one of the prior methods (eg: Petley and Aggidis 2016). Regardless of the method of obtaining the water level, the general assumption is that the external water level is not significantly altered by the operation of the tidal range scheme for these modelling purposes. This is known to be a false assumption; however, the degree of influence is highly dependent on both the physical layout of the scheme, the adjacent bathymetry, and the operational choices made in the control of the scheme. Despite this, there is in the literature a good agreement between 0D and 2D models in terms of estimating the outputs, with the 0D model typically providing a higher output estimate than the 2D modelled equivalent (Harcourt et al., 2019; Xue et al., 2019). For this study, the measured water levels obtained by the British Oceanographic Data Center (BODC) from 2018 at the chosen sites were used, along with an energy sell price record obtained from Elexon (2020). This data was used for both the example schemes to provide a validation output of the model against prior studies with the same control options.

2.2 Imposed Errors

As the purpose of the tests was to determine how a notional error will impact the expected energy or profit generated, the raw time series were mutated to generate these errors. Five simple error modes were identified based on common traits seen in water level series data per Williams and Esteves (2017), exemplified in Figures 3-5 for a simple waveform. Firstly, a random deviation in water surface elevation, as might be seen by a gauging station where wave effects are significant and thus the overall trend is accurate, but the individual points deviate. Secondly, an offset - or datum error, can occur from the improper calculation of relative levels such as when converting between measurement systems at a variety of sites. Third, a 'drifting' error, whereby a deviation between the true and false traces gradually grows, as could be induced by a long-form oceanic effect (such as a tidal surge) or an instrument error. A scaling error where the magnitude of the assumed trace is either too large or small can come from an incorrect modelling assumption to overestimate the tidal amplitude, or the usage of an overly large sample in a moving average (such as to counteract the effects of the first error type). Finally, a temporal issue can be incurred, where the level is correct but mistimed, which will affect how it interacts with other independent sources of information, this can occur for example when a time zone is incorrectly identified. All or some of these error types, along with others, can combine to create new error forms whose identification is more complex.

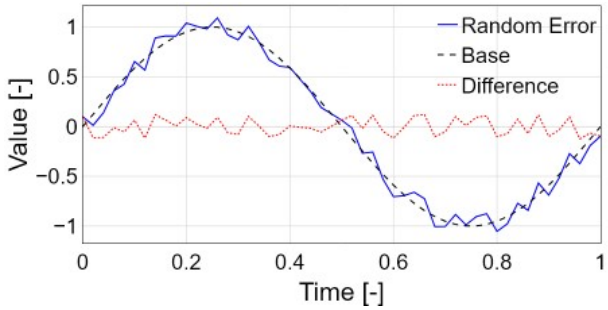

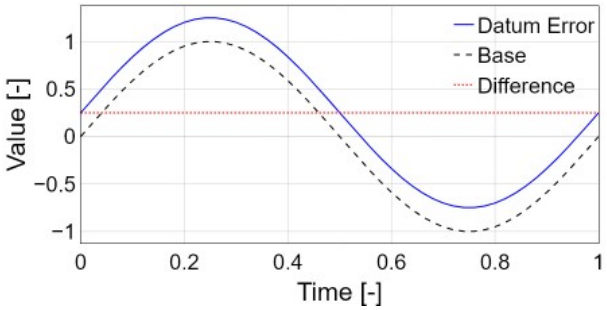

Figure 3. Random and Datum error types applied to waveform

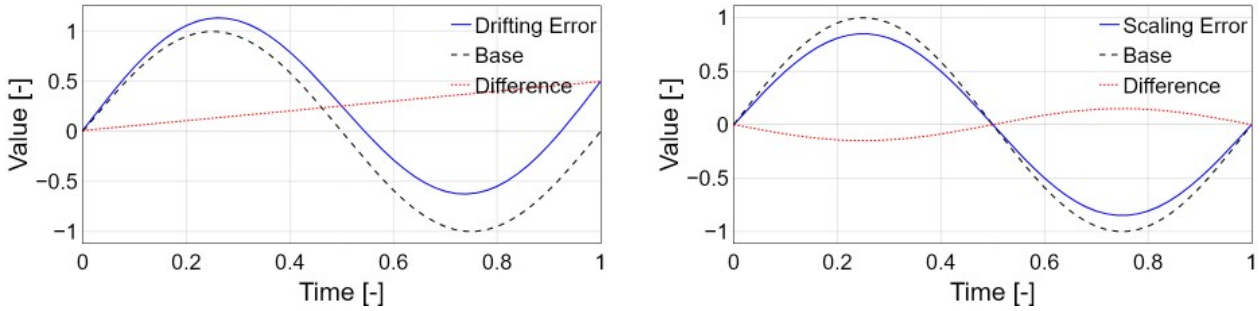

Figure 4. Drifting and scaling errors applied to waveform.

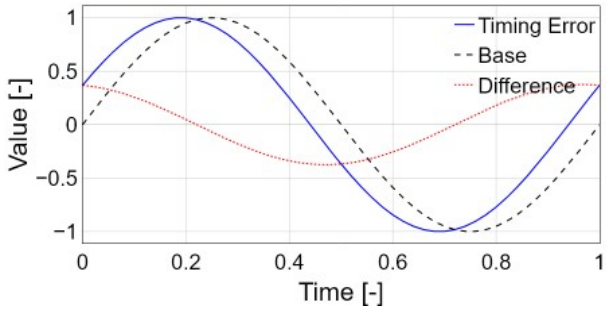

Figure 5. Timing error applied to waveform.

The mutated signal at a time *i*, η^i, is generated based on the input water level z^i with errors applied as shown in Equations 7-11, for a set of *N* points, with the error forcer *X* varying from the relevant X_{min} to X_{max} as shown in Table 2. X has a value of meters, hours, or magnitude.

$$\eta^i_{rng} = z^i + RAND^{X/2}_{-X/2} \quad [7]$$

$$\eta^i_{datum} = z^i + X \quad [8]$$

$$\eta^i_{drift} = z^i + \frac{i}{N}X \quad [9]$$

$$\eta^i_{scale} = z^i \times X \quad [10]$$

$$\eta^i_{timing} = z^{i+X} \quad [11]$$

$$X_{min} \leq X \leq X_{max} \quad [12]$$

Table 2. Error forcer ranges for the mutated time-series.

Error Type	Maximum	Minimum	Units
Random	0.1	2	m
Datum	-1.5	1.5	m
Drift	0.05	0.5	m
Scale	0.5	1.5	-
Timing	0.5	4	hrs

2.3 Statistical Calibration Metrics

Each of the error types are applied to the base time series at a range of magnitudes (size of deviation) and the statistical differences between the two series assessed using selected common parameters. The dimensionless coefficient of determination R^2 Eq. [13], quantifies how well a simulated set of values η_i matches an observed set of values z_i as a comparison to using the mean of the measured data $\bar{z}$, a value of 1.0 indicates a perfect match between measured and observed, 0 being an accuracy equal of that of using the mean of the observed data, and a negative value indicating that the prediction is less useful than the mean. This has been used to calibrate numerical models at given measurement sites by 6 of the sample studies (footnote 1) with a minimum value of 0.86 used by Mejia-Olivares et al. (2020). The Root Mean Square Error (RMSE), shown in

Eq. [14] is a measure of accuracy whereby a value of 0 indicates a perfect fit of the observation z_i and prediction η_i. RMSE is always positive, with a magnitude and units being based on the inputs and a maximum value of 0.53 m presented by (Xia et al., 2010). This is normalised by dividing the RMSE by the mean of the observed data giving the Scatter Index [15], as has been suggested by (Williams and Esteves, 2017) to normalise the RMSE across locations with varying typical conditions. The Mean Absolute Error [16] is the average difference between the prediction and the observation, with units and magnitude to the parameter being investigated, as used by Guo et al. (2021) and Mackie et al. (2021) where a value of ≤ 0.338 m was deemed to be suitable in the calibration of 2D models. Multiple fitness functions are used here to ascertain if a specific choice or combination can offer more insight than the others, and what types of error each is best suited to identifying.

$$R^2 = 1 - \frac{\sum_{i=1}^{N}(z_i - \eta_i)^2}{\sum_{i=1}^{N}(z_i - \bar{z})^2} \quad [13]$$

$$RMSE = \sqrt{\frac{\sum_{i=1}^{N}(z_i - \eta_i)^2}{N}} \quad [14]$$

$$Scatter\ Index = \frac{RMSE}{\bar{z}} \quad [15]$$

$$MAE = \frac{\sum_{i=1}^{N}|(z_i - \eta_i)|}{N} \quad [16]$$

2.4 Studied Schemes

The West Somerset Lagoon proposal and Mersey Tidal Barrage proposal were chosen as case studies due to their relevance and ongoing states of development, for descriptions of the schemes please refer to Neill et al. (2018). For each scheme, there are a variety of operational choices that can be made, whether to operate in one or both directions of flow, open the sluices before/after closing the turbines, use a fixed condition to start and end generation periods, and whether to use the turbines as pumps to increase the yield by forcing the flow to better prepare the water condition for the upcoming phases. In this sample, two study lagoons were operated in a fixed and flexible mode, for both ebb only and two-way generation, using a water level time series with each error mechanism, at a variety of severities. From this, the statistical comparison of the base and mutated time-series data was determined along with the financial output of the scheme when under these conditions. This provides a degree of insight into what operational decisions/configurations are more sensitive to errors in the inputs, thus providing some guidance to users who have lower confidence in their data so can opt for a robust configuration.

To validate the model's ability to match the performance of these schemes in the existing literature, fixed case base conditions were simulated. At the West Somerset lagoon, the 125 Turbine, 20000 m² sluice area design with a starting head difference of 4.9 m, and ending of 2.5 m was modelled from Xue et al. (2021) and found to have a difference of 1.5 % total energy output. The Mersey Barrage configuration presented by Aggidis and Benzon (2013) of 28 turbines and 2592 m² of sluice gates was run with a Start and end head of 3.9 and 1.2 m respectively with the net energy output agreeing to within 2 %. Further base conditions were established to provide the theoretical basis for alternate operation possibilities, the profit generated by the mutated time series is divided by these base values to derive a relative yield.

3. RESULTS AND DISCUSSION

To determine the variability of the profit generated by the scheme (yield) the base energy output was calculated for each scheme under each combination of operating mode (ebb-only and two-way), for both fixed and flexible control. The resulting data was then filtered to remove any simulated time series that had an $R^2 <$ 0.86, and RMSE > 0.53, the boundary levels found in the surveyed literature. This resulted in a total of 248 model runs being retained for analysis. The relative yield distribution of models using the error mechanisms is displayed in **¡Error! No se encuentra el origen de la referencia.**, separated based on fixed and flexible operation. From this, a relatively impactful level of scaling error passed the filter levels and incurred significant variation in the yield, especially in the fixed operation case. The scaling error, although impactful, is relatively predictable, as a larger tidal form gives larger yields, thus an assessment of the mean, minimum and maximum tidal ranges may give a prediction of this error and an indication of the potential over/underestimate of yield. Drift and timing errors were less likely to incur variation if within the bounds and were broadly mitigated when

using fixed operation. The random error form can be seen to have had an overall negative impact on the predicted outputs, likely due to the small deviations triggering start/end points at suboptimal times.

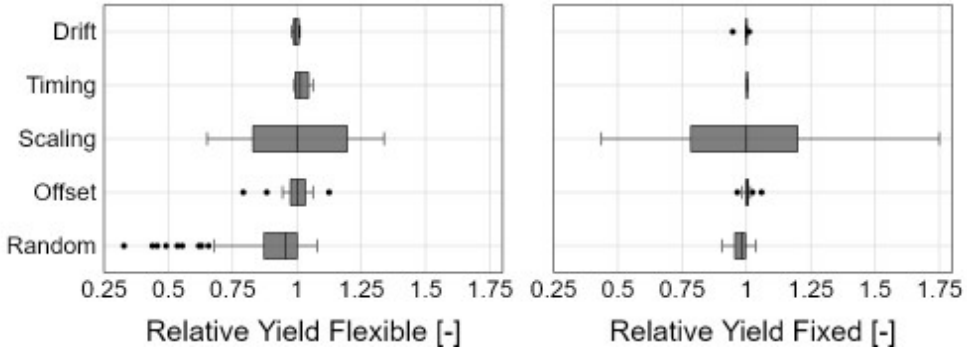

Figure 6. Output distribution of error mechanisms.

When plotted against the R^2, the yield (Figure 7) was seen to quickly vary from the base, whilst some more accurate results demonstrated worse goodness of fit than poorly performing counterparts, indicating that R^2 alone cannot guarantee an accurate result below a very high agreement (approximately 0.999). The RMSE (Figure 7) and scatter index (Figure 8) suggest that as the error metric grows, the variation in outputs also does. For these tests, when the scatter index was less than 0.175 the relative yield was within 5% away of the baseline. The ± 5 % margin is reached when the MAE is below 0.05 m.

To ascertain the degree to which a given operational configuration might be more resistant to errors in the water level, the filtered data points were sorted by operational configuration and the distribution of their relative yields plotted in Figure 9 and Figure 10. For the given schemes, when using the time series data that falls within the identified limits, the variation does not change from operation to operation. Most operating configurations display a skew towards underestimating the yield. This may be due to the nature of the errors causing the control algorithms to activate at suboptimal points, providing a conservative estimate of performance.

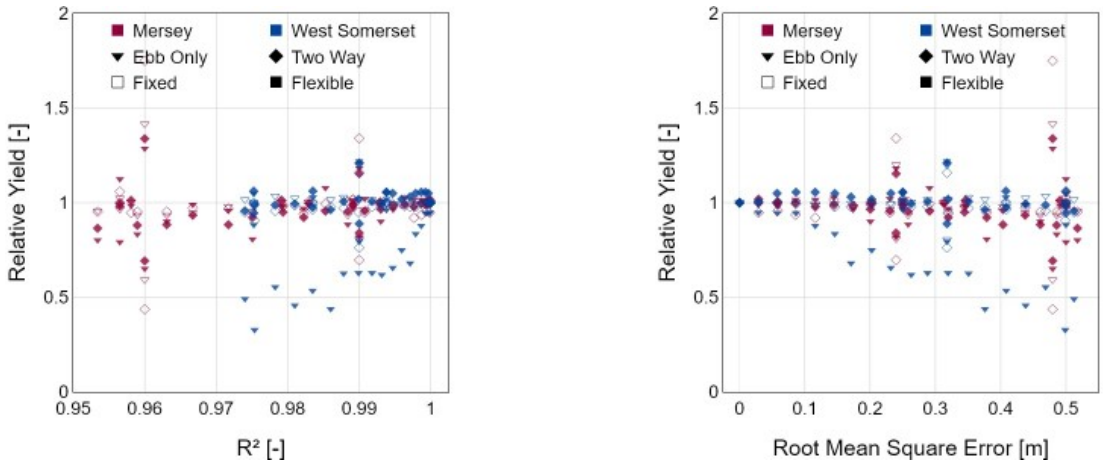

Figure 7. Relative yields plotted against R^2 and RMSE.

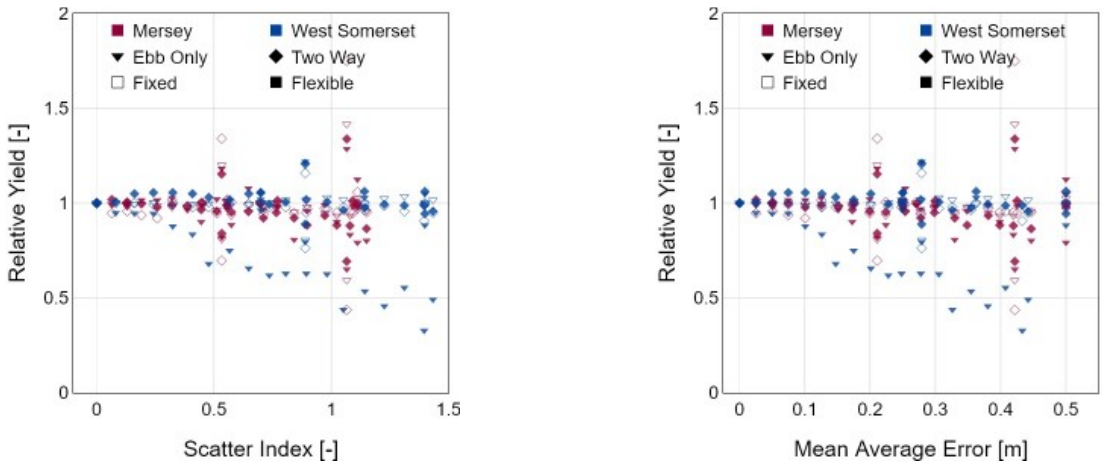

Figure 8. Relative yields plotted against Scatter Index and MAE.

In general, the Mersey model was more sensitive to water level particularly during flexible ebb-only operation, with a greater deviation particularly when operating flexibly in the ebb-only mode. This may have been due to the nature of the water levels at the site, or a function of the number of sluices and turbines in use, future study would benefit from cross-analysing additional sites and their physical characteristics to identify which component of the design allows for the most robust estimates, and how this translates to performance.

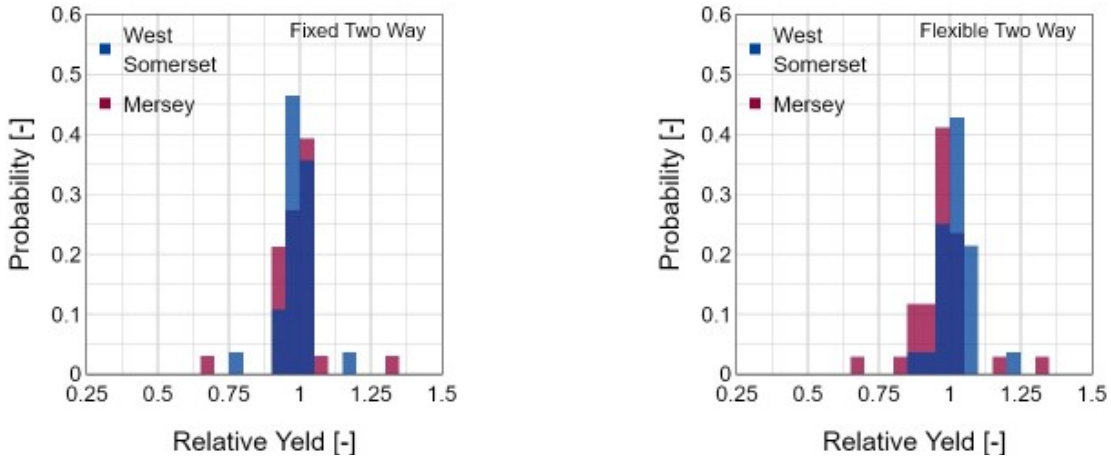

Figure 9. Variations in fixed and flexible control for two-way operation.

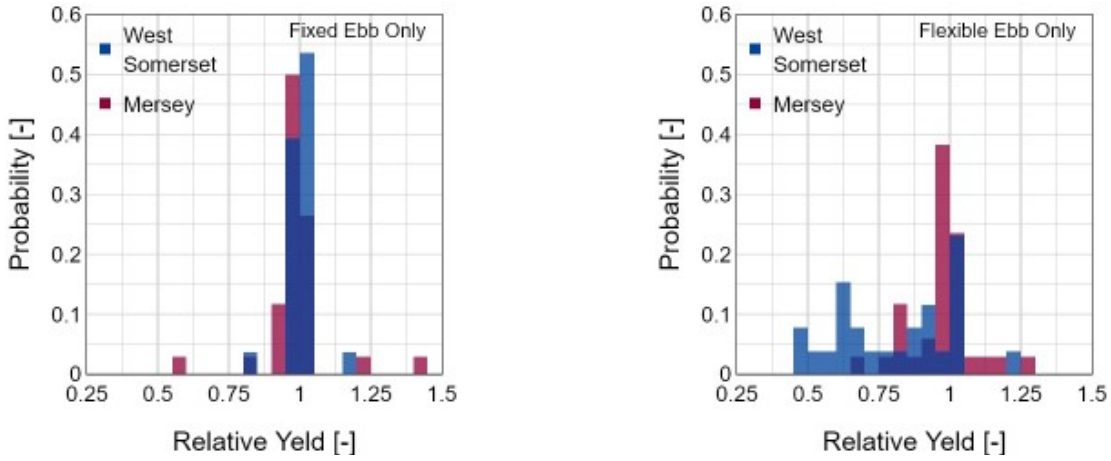

Figure 10. Variations in fixed and flexible control for ebb-only operation.

4. CONCLUSIONS

To determine the ability of some commonly used statistical parameters to detect errors in the input time series for a 0D model of a tidal range scheme, a set of base conditions at multiple sites were established, and then run with a variety of water level sets mutated with synthetic errors. These errors, while not exhaustive provide a variety of mechanisms through which a trace could be inaccurate. A level of error found to be within the used limits of the studied literature can result in a 0D model returning a yield that is significantly greater or smaller than the true value at inopportune configurations. At the two schemes studied, it was found that the random variation error type was most likely to pass within the bounds set by a statistical analysis of the time series data alone but likely to have a negative impact on output. Scaling errors were found to pass the filter and have a significant but predictable effect on the yield of the scheme, particularly so when operating in a fixed mode of operation. In future work a harmonic analysis, or assessment of tidal range statistics may be able to more accurately provide guidelines, building on the guidance of Williams and Esteves (2017). No mode of operation was found to be significantly more resilient to errors in the water levels, however, this is dependent on the scheme configuration and error form itself. This study highlights the importance of using high quality data in the modelling of tidal range energy schemes, It is key to be aware that an mildly erroneous water level is still viable for usage in the design of a tidal range schemes, and comparison between 0D and 2D models has been reported within 5% (Xue et al., 2019). the comparison between modes and operational decisions is often as useful as the raw yield assumption in the developmental stages, and this is less reliant on water level data than other analysis stages.

5. ACKNOWLEDGEMENTS

This work was funded as part of the Water Informatics Science and Engineering Centre for Doctoral Training (WISE CDT) under a grant from the Engineering and Physical Sciences Research Council (EPSRC), grant number EP/L016214/1.

6. REFERENCES

Aggidis G.A., and Benzon D.S. (2013) Operational optimisation of a tidal barrage across the Mersey estuary using 0-D modelling. *Ocean Engineering*, 66:69–81.

Aggidis G.A., and Feather O. (2012) Tidal range turbines and generation on the Solway Firth. *Renewable Energy*, 43:9–17.

Ahmadian R., and Hanousek N. (2021) Exploring broader benefits of tidal range schemes. Hydrolink 79–82

Angeloudis A., Ahmadian R., Falconer R.A., and Bockelmann-Evans B. (2016) Numerical model simulations for optimisation of tidal lagoon schemes. *Applied Energy*, 165:522–536.

Angeloudis A., Kramer S.C., Avdis A., and Piggott M.D. (2018) Optimising tidal range power plant operation. *Applied Energy*, 212:680–690.

Čož N., Ahmadian R., and Falconer R.A. (2019) Implementation of a Full Momentum Conservative Approach in Modelling Flow Through Tidal Structures. *Water*, 11:1917.

Elexon. (2020) Electricity Pricing. In: Elexon Knowl. Base. https://www.elexon.co.uk/knowledgebase/where-can-i-find-details-of-wholesale-prices-of-electricity-in-great-britain/

Ghaedi A., and Gorginpour H. (2021) Generated power enhancement of the barrage type tidal power plants. *Ocean Engineering*, 226:108787.

Guo B., Ahmadian R., and Falconer R.A. (2021) Refined hydro-environmental modelling for tidal energy generation: West Somerset Lagoon case study. *Renewable Energy*, 179:2104–2123.

Harcourt F., Angeloudis A., and Piggott M.D. (2019) Utilising the flexible generation potential of tidal range power plants to optimise economic value. *Applied Energy*, 237:873–884.

Mackie L., Kramer S.C., Piggott M.D., and Angeloudis A. (2021) Assessing impacts of tidal power lagoons of a consistent design. *Ocean Engineering*, 240:109879.

Mejia-Olivares C.J., Haigh I.D., Angeloudis A., et al. (2020) Tidal range energy resource assessment of the Gulf of California, Mexico. *Renewable Energy*, 155:469–483.

Moreira T.M., de Faria J.G., Vaz-de-Melo P.O.S., et al. (2022) Prediction-free, real-time flexible control of tidal lagoons through Proximal Policy Optimisation: A case study for the Swansea Lagoon. *Ocean Engineering*, 247:110657.

Neill S.P., Angeloudis A., Robins P.E., et al. (2018) Tidal range energy resource and optimization – Past perspectives and future challenges. *Renewable Energy*, 127:763–778.

Petley S., and Aggidis G.A. (2016) Swansea Bay tidal lagoon annual energy estimation. *Ocean Engineering*, 111:348–357.

Rehman S., Al-Hadhrami L.M., and Alam M.M. (2015) Pumped hydro energy storage system: A technological review. *Renewable and Sustainable Energy Reviews*, 44:586–598.

Rtimi R., Sottolichio A., and Tassi P. (2021) Hydrodynamics of a hyper-tidal estuary influenced by the world's second largest tidal power station (Rance estuary, France). *Estuarine, Coastal and Shelf Science*, 250

Swansea Council. (2021) £1.7 billion Blue Eden project announced for Swansea. https://www.swansea.gov.uk/BlueEden. Accessed 17 Nov 2021

Todeschini G., Coles D., Lewis M.J., et al. (2021) Medium-term variability of the UK's combined tidal energy resource for a net-zero carbon grid. *Energy*, 238:121990.

Waters S., and Aggidis G.A. (2016) A World First: Swansea Bay Tidal lagoon in review. *Renewable and Sustainable Energy Reviews*, 56:916–921.

Williams J.J., and Esteves L.S. (2017) Guidance on Setup, Calibration, and Validation of Hydrodynamic, Wave, and Sediment Models for Shelf Seas and Estuaries. *Advances in Civil Engineering*, 2017

Xia J., Falconer R.A., and Lin B. (2010) Impact of different tidal renewable energy projects on the hydrodynamic processes in the Severn Estuary, UK. *Ocean Modelling*, 32:86–104.

Xue J., Ahmadian R., and Falconer R.A. (2019) Optimising the operation of tidal range schemes. *Energies*, 12:2870.

Xue J., Ahmadian R., Jones O., and Falconer R.A. (2021) Design of tidal range energy generation schemes using a Genetic Algorithm model. *Applied Energy*, 286:116506.

Zhou J., Pan S., and Falconer R.A. (2014) Effects of open boundary location on the far-field hydrodynamics of a Severn Barrage. *Ocean Modelling*, 73:19–29.